Journal of Neuroinflammation

RESEARCH Open Access

Th17 and effector CD8 T cells relate to disease progression in amyotrophic lateral sclerosis: a case control study

Tatsuo Itou[1†], Koji Fujita[2*†], Yuumi Okuzono[1], Dnyaneshwar Warude[1], Shuuichi Miyakawa[1], Yoshimi Mihara[2], Naoko Matsui[2], Hiroyuki Morino[3], Yusuke Kikukawa[1] and Yuishin Izumi[2]

Abstract

The immune system has garnered attention due to its association with disease progression in amyotrophic lateral sclerosis (ALS). However, the role of peripheral immune cells in this context remains controversial. Here, we conducted single-cell RNA-sequencing of peripheral blood mononuclear cells to comprehensively profile immune cells concerning the rate of disease progression in patients with ALS. Our analysis revealed increased frequencies of T helper 17 cells (Th17) relative to regulatory T cells, effector CD8 T cells relative to naïve CD8 T cells, and $CD16^{high}CD56^{low}$ mature natural killer cells relative to $CD16^{low}CD56^{high}$ naïve natural killer cells in patients with rapidly progressive ALS. Additionally, we employed serum proteomics through a proximity extension assay combined with next-generation sequencing to identify inflammation-related proteins associated with rapid disease progression. Among these proteins, interleukin-17 A correlated with the frequency of Th17, while killer cell lectin-like receptor D1 (CD94) correlated with the frequency of effector CD8 T cells. These findings further support the active roles played by these specific immune cell types in the progression of ALS.

Keywords Amyotrophic lateral sclerosis, Disease progression, Effector CD8 T cells, Interleukin-17A, Killer cell lectin-like receptor D1 (CD94), Natural killer cells, Single-cell RNA-sequencing, T helper 17 cells

Background

Amyotrophic lateral sclerosis (ALS) is a neurodegenerative disease that affects both upper and lower motor neurons [1]. Following the onset of symptoms, muscle weakness relentlessly progresses, eventually leading to respiratory failure and, unfortunately, death within a few years for most patients. Nonetheless, the rate of progression varies considerably among patients [1]. This variability in progression poses a challenge toward the development of therapeutics because clinical trials for ALS typically assess progression as the primary outcome [2]. Therefore, gaining deep understanding on the pathogenesis of disease progression in ALS is of utmost importance.

†Tatsuo Itou and Koji Fujita contributed equally to this work.

*Correspondence:
Koji Fujita
kfujita@tokushima-u.ac.jp
[1]Oncology Drug Discovery Unit Japan, Pharmaceutical Research Division, Takeda Pharmaceutical Company Limited, Fujisawa, Japan
[2]Department of Neurology, Tokushima University Graduate School of Biomedical Sciences, Tokushima, Japan
[3]Department of Medical Genetics, Tokushima University Graduate School of Biomedical Sciences, Tokushima, Japan

The progression of ALS has been linked to immune cells and proteins in both the central nervous system (CNS) and peripheral circulation [3, 4]. However, several critical questions in this regard remain unanswered. For instance, a decrease or dysfunction in regulatory T cells (Treg), characterized by the expression of the FOXP3 transcription factor, has been correlated with rapid progression [5–8]. Furthermore, a flow cytometric study has reported that reduced levels of peripheral CD4 T cells are associated with the rate of progression, with the assumption that the reduction is linked to decreased Treg levels, although subpopulations of the peripheral blood CD4 T cells were not specifically examined [8]. Conversely, another flow cytometric study demonstrated that ALS patients with higher levels of CD4+FOXP3− effector T cells in the cerebrospinal fluid (CSF) exhibited a higher rate of progression; although, detailed profiles of the CD4 T cell subpopulations were unavailable [9]. Therefore, the roles of CD4 T cell subpopulations, other than Treg, in disease progression remain enigmatic in ALS.

Additionally, although an increase in CD8 T cells has been reported in ALS [10, 11], the function of CD8 T cells in disease progression remains unknown. Furthermore, studies investigating pro and anti-inflammatory cytokines in the blood of ALS patients, primarily based on enzyme-linked immunosorbent assays, have failed to detect correlations between cytokine levels and the Revised Amyotrophic Lateral Sclerosis Functional Scale (ALSFRS-R), which is used to assess disease severity and progression [12–17].

To address these unresolved issues, we conducted an unbiased evaluation of phenotypes in peripheral blood immune cells, encompassing not only CD4 T cells but also CD8 T cells and natural killer (NK) cells, in patients with ALS and healthy subjects. We assessed their association with the rate of progression in patients with ALS through single-cell RNA-sequencing (scRNA-seq) of peripheral blood mononuclear cells (PBMCs) [18–20]. We also analyzed differentially expressed genes (DEG) in the scRNA-seq data. Furthermore, we searched for inflammation-related proteins in the serum linked to progression using a proximity extension assay (PEA) in conjunction with a high-throughput sequencing read-out [21, 22]. Considering reproducibility, major findings of the PEA were tested with Single molecule array (Simoa). We aimed to elucidate the interplay between immune cells and proteins in the context of disease progression in ALS.

The scRNA-seq analysis highlighted the involvement of T helper 17 cells (Th17), effector CD8 T cells, and $CD16^{high}CD56^{low}$ mature NK cells, while PEA identified associated proteins such as interleukin-17 A (IL-17 A) and killer cell lectin-like receptor D1 (KLRD1, also known as CD94), in relation to the rapid progression of ALS. CD94, expressed on NK cells and a small subset of CD8 T cells, forms a heterodimer with NKG2. The CD94/NKG2 receptor complex recognizes nonclassical MHC class I molecules, including HLA-E in humans and Qa-1 in mice, and has established roles in tumor immunity, viral infection, and autoimmunity [23–25]. Meanwhile, DEG analysis revealed downregulation in SERPINA1 and AC103591.3 (RP11-386I14) in patients with ALS. SerpinA1, a serine protease inhibitor, is implicated in modulating microglial-mediated inflammation in neurodegenerative diseases [26]. RP11-386I14, a long non-coding RNA expressed in B cells, monocytes, T cells, and NK cells [27], remains functionally uncharacterized. Together, these findings provide novel insights into peripheral immune mechanisms involved in the progression of ALS.

Results

Participants

Of the 46 screened participants, 10 healthy controls and 35 patients with ALS gave informed consent, and one participant with neuropathy was excluded. Additionally, five participants with ALS who had gastric cancer ($n=1$), hepatocellular carcinoma ($n=1$), human T-lymphotropic virus type 1 antibody ($n=1$), *SOD1* ($n=1$), and lung cancer and *SOD1* ($n=1$) were excluded because they met one or two of the exclusion criteria, such as persons with malignant tumors, persons with diseases in which immune abnormality is involved in the onset of the disease (e.g., autoimmune diseases), and patients with known pathogenic ALS variants (see Materials and Methods). Eventually, peripheral blood samples of 10 healthy controls (age, 63.6±10.2; male, 7), 23 patients with non-rapid ALS (ΔALSFRS-R/month<1; age, 60.7±10.8; male, 17), and 7 patients with rapid ALS (ΔALSFRS-R/month≥1; age, 69.8±14.4; male, 3) were analyzed (Table 1). Patients with ALS had disease duration of 10.4±6.4 months and a mean ALSFRS-R score of 39.9±5.2. The clinical information was compared with scRNA-seq and proteomics data (Fig. 1A).

Single-cell RNA-sequencing

The integrated scRNA-seq classified the cells into 23 types for further analysis (Fig. 1B, S1). The number of cells in each cell subset is shown in Table S1. We first calculated the frequencies of cell types in all cells in healthy control, non-rapid ALS, and rapid ALS (Fig. 1C, S2). The number of Treg significantly increased in non-rapid ALS compared with control and rapid ALS (2.4% vs. 1.9%, $p=0.01$ and 2.4% vs. 1.6%, $p=0.03$, respectively; Fig. 2A). Next, we calculated the frequencies of cell types in related cells. The frequency of effector CD8 T cells in all CD8 T cells was significantly higher in rapid than non-rapid ALS (91.6% vs. 82.2%, $p=0.04$). In contrast, the frequency

Table 1 Clinical features of 40 subjects

	Healthy control (*n* = 10)	Non-rapid ALS (*n* = 23)	Rapid ALS (*n* = 7)
Age, years, mean ± SD	63.6 ± 10.2	60.7 ± 10.8	69.8 ± 14.4
Male, N (%)	7 (70.0)	17 (73.9)	3 (42.9)
ALSFRS-R at entry, mean ± SD	-	41.8 ± 2.6	34.7 ± 7.1
Duration before entry, months, mean ± SD	-	12.4 ± 6.2	5.0 ± 2.5
ΔALSFRS-R/month, mean ± SD	-	0.56 ± 0.22	2.81 ± 1.27
Site of onset, N (%)			
Bulbar	-	8 (34.8)	2 (28.6)
Limb	-	14 (60.9)	5 (71.4)
Trunk	-	1 (4.3)	0 (0.0)
%forced vital capacity, mean ± SD	-	87.6 ± 22.7	61.5 ± 41.0
Cognitive status, N (%)			
Normal	10 (100.0)	21 (91.3)	4 (57.1)
Impaired	-	2 (8.7): FTD, 2	3 (42.9): FTD, 1; suspicion of FTD, 1; unknown etiology, 1

ALS: amyotrophic lateral sclerosis; ALSFRS-R: Revised Amyotrophic Lateral Sclerosis Functional Rating Scale; FTD: frontotemporal dementia; SD: standard deviation

of regulatory B cells among all B cells (5.5% vs. 7.3%, $p=0.05$) and those of naïve and exhausted CD8 T cells among all CD8 T cells (4.1% vs. 8.4%, $p=0.01$ and 0.6% vs. 0.9%, $p=0.04$, respectively) were significantly lower in rapid than non-rapid ALS (Fig. 2B). Furthermore, we calculated the frequency ratios between functionally related immune cells. The ratios of memory CD4 T cells/Treg (4.9 vs. 2.9, $p=0.02$), Th1/Treg (1.9 vs. 1.2, $p=0.02$), Th17/Treg (1 vs. 0.6, $p=0.005$), effector/naïve CD8 T cells (23.0 vs. 9.8, $p=0.01$), effector/exhausted CD8 T cells (149.7 vs. 89.9, $p=0.02$), and mature ($CD16^{high}CD56^{low}$)/naïve ($CD16^{low}CD56^{high}$) NK cells (28.1 vs. 20.1, $p=0.04$) were significantly higher in rapid than non-rapid ALS (Fig. 2C).

Cell type frequencies and progression rate

We investigated the relationship between cell type frequencies and progression rate in ALS. We used partial correlation because ΔALSFRS-R/month was correlated with age (Pearson's correlation coefficient = 0.421, $p=0.02$), and confounding with age could not be ignored in routine correlation analysis. The frequency of Th17 in CD4 T cells significantly correlated with ΔALSFRS-R/month (coefficient = 0.390, $p=0.037$). Moreover, the ratios of memory CD4 T cells/Treg (coefficient = 0.450, $p=0.014$) and Th17/Treg (coefficient = 0.428, $p=0.021$) moderately but significantly correlated with ΔALSFRS-R/month (Fig. S3, Tables S2–4).

Differentially expressed genes

We performed DEG analysis of scRNA-seq data between ALS versus control, non-rapid ALS versus control, rapid ALS versus control, and rapid ALS versus non-rapid ALS, and then isolated the DEGs in 23 cell types (Bonferroni adjusted $p<0.05$, fold change [FC] ≥ 1.2). SERPINA1 in naïve CD4 T cell and AC103591.3 in classical monocytes were downregulated in ALS than in control but were not different between rapid and non-rapid ALS (Table S5).

Inflammation proteins

PEA-based proteomics of serum identified KLRDD1 (CD94) (FC = 2.2, $p<0.001$), trefoil factor 2 (TFF2; FC = 2.3, $p<0.001$), keratin, type I cytoskeletal 19 (KRT19; FC = 3.2, $p<0.001$), IL-17 A (FC = 4.8, $p=0.007$), YTH domain-containing family protein 3 (YTHDF3; FC = 2.6, $p=0.03$), and neutrophil cytosolic factor 2 (NCF2; FC = 2.4, $p=0.04$) as significantly elevated in rapid versus non-rapid ALS. Of these, KLRD1 (FC = 2.2, $p<0.001$), KRT19 (FC = 2.7, $p=0.01$), NCF2 (FC = 3.0, $p=0.02$), YTHDF3 (FC = 3.0, $p=0.02$), and IL-17 A (FC = 4.0, $p=0.04$) were significantly elevated in rapid ALS than in control (Fig. 3A, B). IL-17 A concentrations measured with Simoa were also significantly higher in rapid ALS than in non-rapid ALS ($p=0.04$, Tukey's honestly significant difference [HSD] test; $p=0.04$, one-way ANOVA) (Fig. S4). Expression levels of phosphorylated neurofilament heavy chain (pNfH) were significantly higher in ALS (non-rapid + rapid) than in control (FC = 180, $p=0.001$) and in rapid ALS than in control (FC = 3074, $p<0.001$) (Fig. 3A, C), which supported the validity of our samples.

Moreover, we conducted a partial correlation analysis between serum protein levels and ΔALSFRS-R/month to examine whether the measured proteins correlated with the progression rate (Table S6). All the six differentially expressed proteins (DEPs) that were elevated in rapid ALS versus non-rapid ALS had significant correlations, especially KLRD1 (coefficient = 0.745, $p<0.0001$), KRT19 (coefficient = 0.658, $p=0.0002$), and IL-17 A (coefficient = 0.556, $p=0.003$), with partial correlation coefficients of > 0.5 and p-values of ≤ 0.003. In parallel, we also detected CD160, which is associated with NK and CD8 T cells with cytolytic effector activity, as highly correlated with disease progression.

Correlation between proteins and cell types

We investigated the correlation between the serum protein levels and the cell type ratios obtained by the scRNA-seq (Table S7). Regarding the proteins elevated in rapid versus non-rapid ALS, NCF2–classical monocyte/all cells, IL-17 A–memory CD4 T cells/CD4 T cells, IL-17 A–Th17/CD4 T cells, TFF2–effector CD8 T cells/CD8 T cells, KLRD1–effector CD8 cells/CD8 cells, and

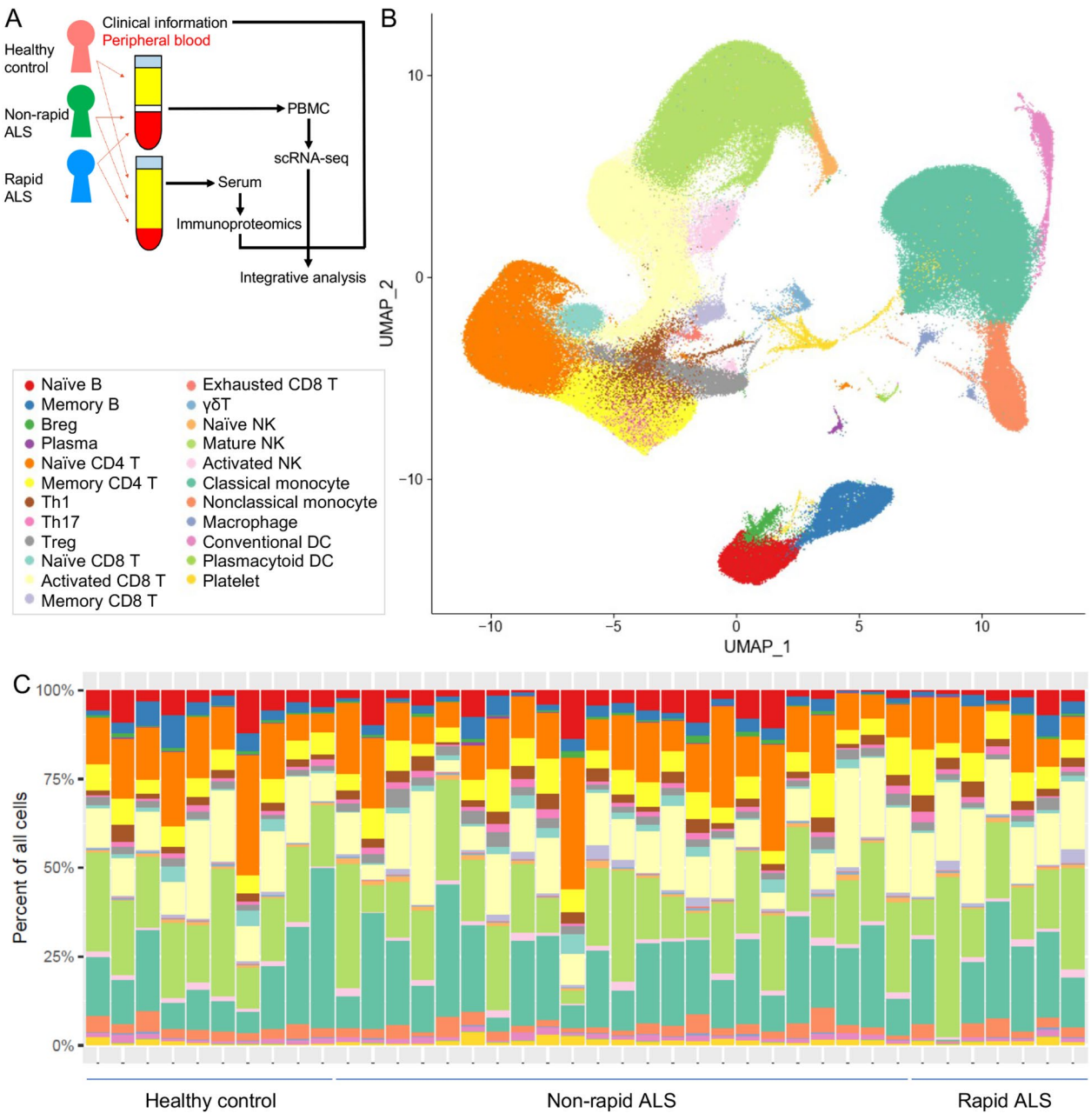

Fig. 1 Study design and profiling of cell types in single-cell RNA-sequencing. **(A)** Overview of this study integrating single-cell RNA-sequencing (scRNA-seq) analysis of peripheral blood mononuclear cells (PBMCs), serum proteomics, and clinical information for healthy controls and patients with non-rapid and rapid amyotrophic lateral sclerosis (ALS). **(B)** Uniform manifold approximation and projection (UMAP) showing 23 identified cell types. **(C)** The frequencies of cell types for each sample. The frequency is displayed as the percentage of each cell type when the total number of cells in each sample was 100%. DC: dendritic cell; NK: natural killer

KLRD1−effector CD8 T cells/exhausted CD8 T cells were the significant combinations with correlation coefficients of >0.5 (Fig. 4). In addition, the ratio of effector CD8 T cells correlated with tumor necrosis factor receptor superfamily member 11B, which also correlated with ΔALSFRS-R/month (partial correlation coefficient=0.402, p=0.031).

Discussion

This study applied multiomics to blood profiling and determined how immune changes relate to disease progression in patients with ALS. The scRNA-seq uncovered cell type shifts from Treg toward Th17, naïve toward effector CD8 T cells, and naïve toward mature NK cells in rapidly progressive ALS. The serum proteomics revealed that IL-17 A and KLRD1 (CD94) increased in rapidly

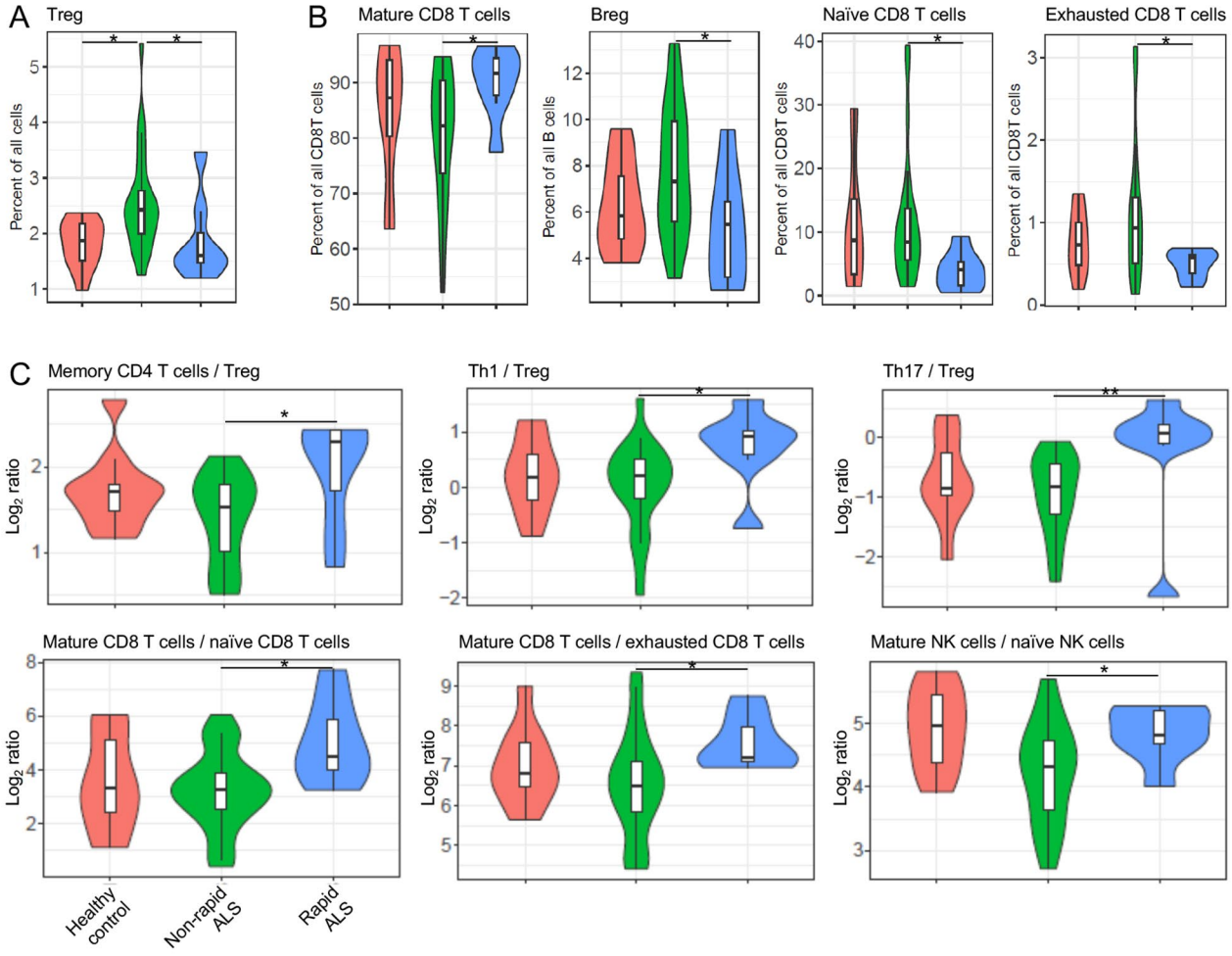

Fig. 2 Intergroup comparison of frequencies of each cell type. **(A)** Frequencies of regulatory T cells in all cells. **(B)** Frequencies of cell types in specific cell groups. **(C)** Ratios of cell types compared to related cell types. They revealed significant differences in rapid amyotrophic lateral sclerosis (ALS) compared to non-rapid ALS by Tukey's HSD test. Lines and asterisks show significant combinations by Tukey's HSD test (*$p < 0.05$, **$p < 0.005$, and ***$p < 0.0005$). Breg: regulatory B cells; NK: natural killer; Th1: T helper 1 cells; Th17: T helper 17 cells; Treg: regulatory T cells

progressive ALS and correlated with frequencies of Th17 and effector CD8 T cells, respectively, thus reinforcing the active roles of these cell types.

Th17 can promote protective immunity against many pathogens but also drive inflammatory pathology during infection, autoimmunity such as multiple sclerosis, and neurodegeneration such as Alzheimer's [28]. Flow cytometric analyses using PBMCs revealed ALS patients had higher frequencies of Th1 and Th17 and lower frequencies of Th2 and Treg compared with healthy controls [13, 14]. However, previous studies showed no relationship between Th17 and disease progression. Similarly, an increase in IL-17 A, the major effector cytokine of Th17, was reported in serum or CSF in ALS patients [13–17]. However, the association between IL-17 A and disease progression remained unknown. Here, we successfully related not only Th17 but also IL-17 A to the rapid progression of ALS. The results regarding IL-17 A were reproduced by measurement with Simoa.

Notably, effector CD8 T cells, compared to naïve CD8 T cells, have also emerged as a phenotype associated with the rapid progression of ALS. CD8 T cells have been reported to play significant roles in SOD1-ALS and juvenile ALS-4, which is caused by SETX mutation [29–31]. In SOD1 model mice, the depletion of CD8 T cells led to an increase in the number of surviving motor neurons, whereas CD8 T cells expressing mutant *SOD1* were found to selectively recognize and kill motor neurons in vitro [30]. More recently, in *SETX* knock-in mice with the L389S mutation, T cell receptor (TCR) repertoire analysis of both the CNS and blood revealed the presence of clonally expanded PD-1+CD8 T cells [31]. These expanded PD-1+CD8 T cells were associated with immunity to glioma but not melanoma, suggesting their recognition of antigens of CNS origin. Additionally, clonally expanded,

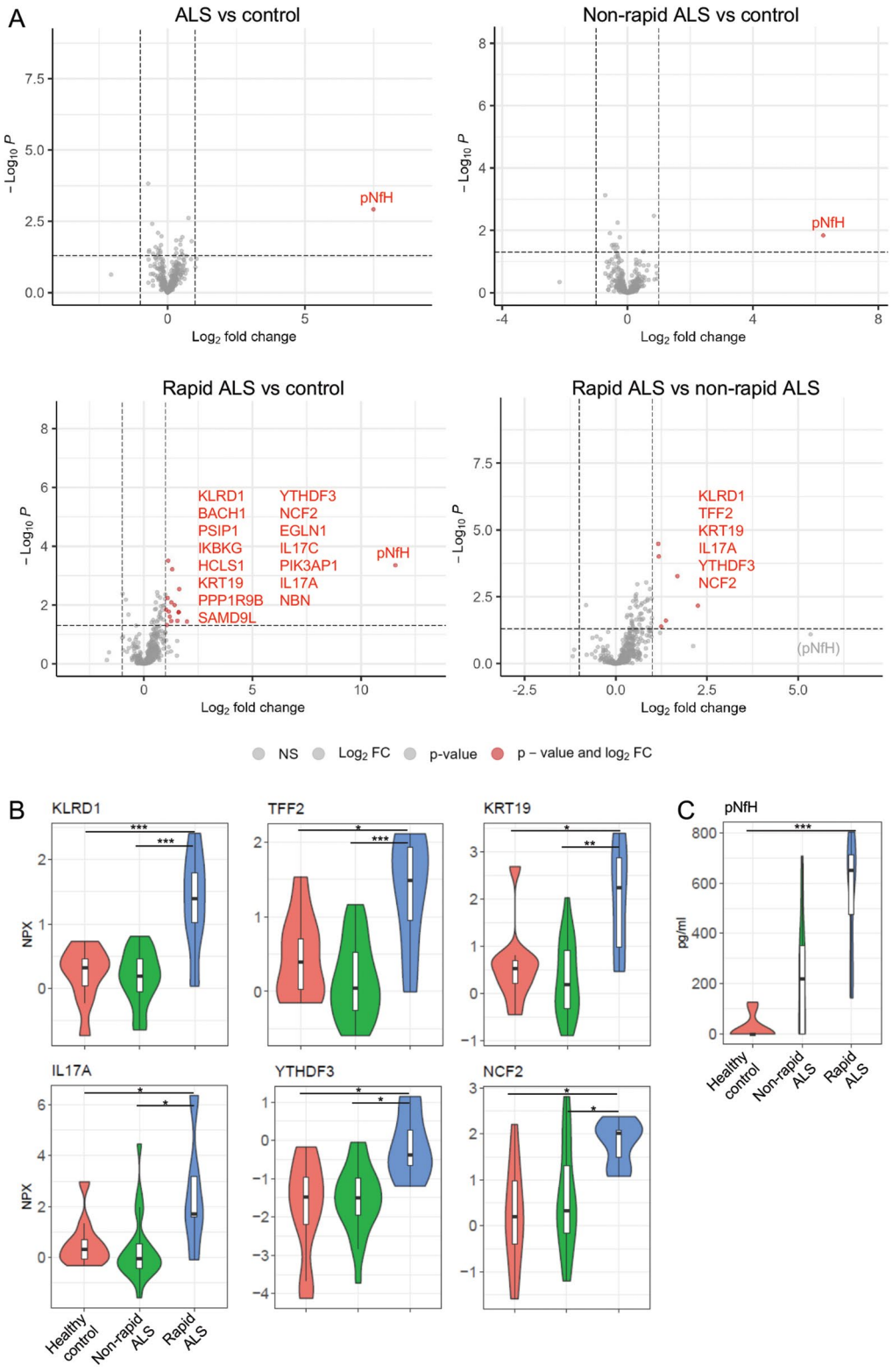

Fig. 3 Serum proteomics. **(A)** Volcano plots showing $-\log_{10}p$-values and $\log_2$ fold changes from differential expression analysis. Red dots indicate differentially expressed proteins (DEPs) shown in gene names. **(B)** Violin plots showing normalized protein expression (NPX) values for six proteins isolated as DEPs with rapid versus non-rapid amyotrophic lateral sclerosis (ALS). **(C)** Violin plots showing expression levels for phosphorylated neurofilament H (pNfH). Lines and asterisks show significant combinations by Tukey's HSD test (*$p < 0.05$, **$p < 0.005$, and ***$p < 0.0005$)

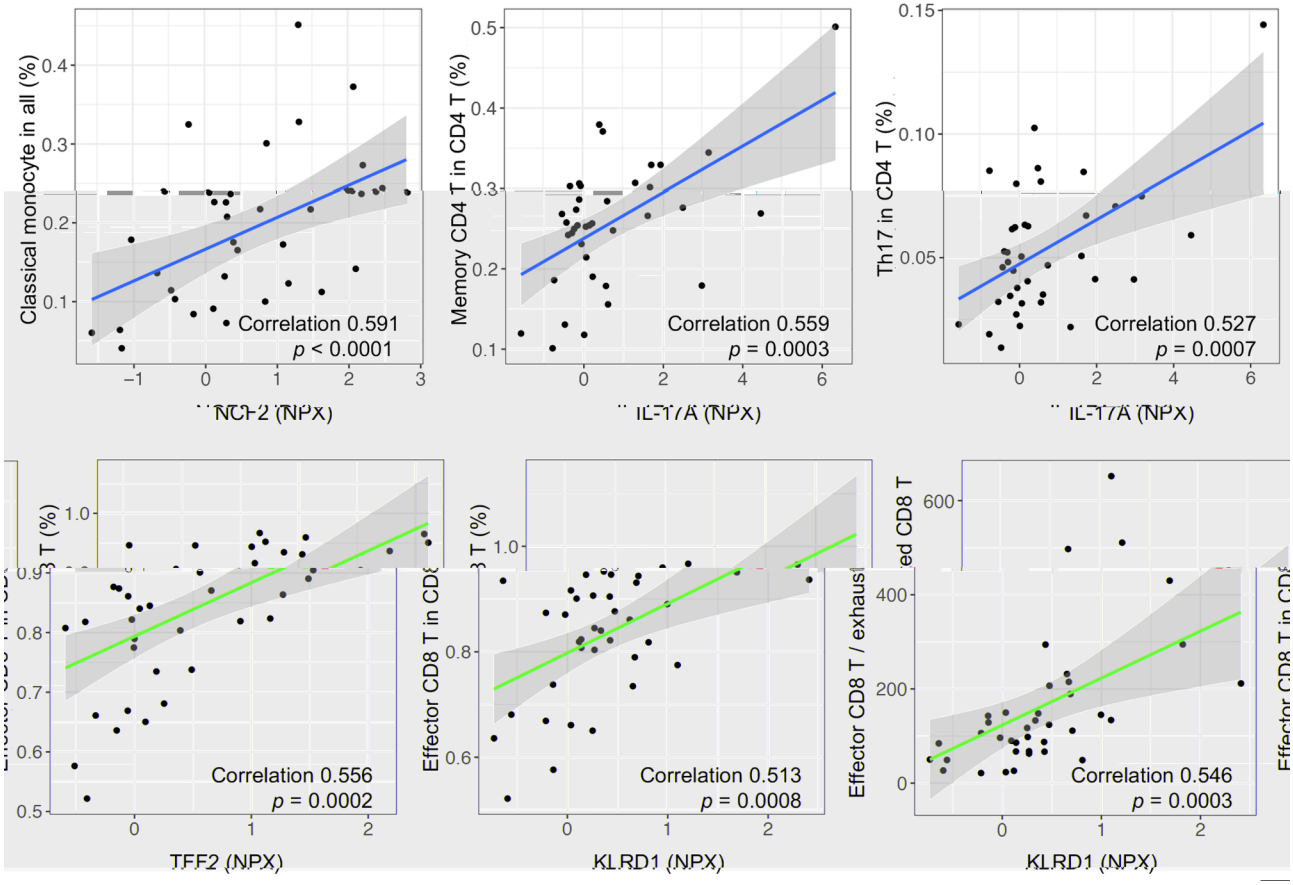

Fig. 4 Correlation between serum proteins and ratios of cell types. Scatter plot between the normalized protein expression (NPX) of serum proteins and the cell frequencies or ratios in single-cell RNA-sequencing analysis using Pearson's correlation coefficient. Numerical values show the correlation coefficient using samples from 30 patients with amyotrophic lateral sclerosis and 10 healthy controls

terminally differentiated effector memory CD8 T cells were detected in the peripheral blood of patients with ALS4. These findings indicate that antigen-specific CD8 T cell responses are involved in the pathogenesis of ALS4. Consistent with this, scRNA-seq of CSF showed higher levels of TCR expansions in effector CD4 and CD8 T cells in five ALS patients compared to four disease controls [9]. Together, these findings and our own suggest that effector CD8 T cells in the blood may recognize specific antigens, possibly self-antigens, in ALS patients.

The present and previous findings together suggest that the changes in peripheral immune cell profiles we observed, although they appear modest, are related to distinct disease conditions including progression rates. In a study using flow cytometry [5], like in the present study using scRNA-seq, the frequencies of Treg were higher in non-rapid ALS than in healthy control (1.0% versus 0.4–0.6%) but were similar between rapid ALS and healthy control. In addition, another study showed that Treg ratio was inversely correlated with the progression rate in ALS patients [7], which is consistent with our findings of a lower Treg ratio in rapid ALS. On the other hand, previous studies reported no relationship between the frequency of CD8 T cells and ALSFRS-R scores [10]. In contrast, our study further analyzed the subpopulation of CD8 T cells and revealed opposite trends for effector and naïve CD8 T cells between rapid and non-rapid ALS, suggesting the superiority of our methods.

KLRD1 (CD94), which was associated with the rate of progression and the frequency of effector and naïve CD8 T cells, forms a heterodimer with NKG2. The CD94/NKG2 complex can function as an inhibitor or activator, depending on the specific NKG2 isoforms. For instance, CD94/NKG2A acts as an inhibitory receptor, whereas CD94/NKG2C acts as an activating receptor. Consequently, CD94/NKG2 may regulate the effector functions and survival of NK cells and CD8 T cells. CD94/NKG2A primarily counteracts TCR signaling in a subset of memory/effector CD8 T cells as part of an antigen-driven response to prevent autoimmunity [32]. Conversely, CD94/NKG2C can activate T cells, inducing proliferation and the killing of HLA-E-transfected target cells that lack expression of other MHC-I molecules, even without TCR stimulation. Thus, it constitutes an alternative activation

pathway for a subset of CD8 T cells [33]. In light of these findings, it is crucial to investigate the characteristics of CD94/NKG2 in ALS. Furthermore, our correlation analysis suggests that CD94 may serve as a marker of CD8 T cell activation in ALS, similar to other instances [25].

We found that the ratio of $CD16^{high}CD56^{low}$ mature NK cells to $CD16^{low}CD56^{high}$ naïve NK cells was significantly higher in rapid than non-rapid ALS. It was reported that ALS patients with slower disease progression showed increased proportions of immune-regulatory $CD56^{bright}$ NK cells in the CSF compared with ALS patients with rapid disease progression [11]. Patients with rapid disease progression showed enhanced differentiation of intrathecal $CD56^{bright}$ into $CD56^{dim}$ NK cells, likely accounting for their reduced frequencies in the CSF of these patients [11]. It was also reported that $CD56^{bright}$ NK cells play a role in regulating activated T cells in both the periphery and CSF, thereby attenuating adaptive immune responses and exerting protective effects in autoimmune diseases of the CNS [34]. These findings highlight the relevance of NK cell differentiation to the pathophysiology of ALS.

Our DEG analysis identified downregulation of SERPINA1 in naïve CD4 T cells and AC103591.3 (RP11-386I14) in classical monocytes in ALS patients compared to controls, with no significant differences between rapid and non-rapid ALS groups. This aligns with a recent study [26] reporting decreased serum SerpinA1 in ALS patients and elevated CSF levels in fast progressors, suggesting compartmentalized dysregulation of SerpinA1. A serine protease inhibitor with anti-inflammatory and neuroprotective properties, SerpinA1 modulates CNS inflammation, a key driver of ALS. Reduced serum levels may reflect systemic inflammation or impaired production, compromising its protective effects on naïve CD4 T cells, while elevated CSF levels in fast progressors could represent compensatory upregulation due to CNS neuroinflammation. These alterations may disrupt T cell differentiation and exacerbate immune dysregulation in ALS. Further studies are needed to clarify the mechanisms underlying SERPINA1 dysregulation and its role in disease progression.

On the other hand, information on the role of RP11-386I14 in ALS is scarce. Regarding monocytes, it was reported that the ratio of classical to non-classical monocytes was elevated in patients with ALS [35]. However, the association between monocytes and progression rate was not shown. We showed that the frequency of classical monocytes was correlated with the value of NCF2, which was elevated in rapid versus non-rapid ALS. NCF2 is responsible for the synthesis of superoxide in neutrophils and was reported as one of the ferroptosis- and iron metabolism-related genes differentially expressed in ALS compared to control [36]. These findings suggest that the roles of monocytes in the pathophysiology of ALS warrant further investigation.

Several limitations were noted in this study. First, the number of participants was relatively small; the number was similar to or smaller than those in other studies using flow cytometry or ELISA in patients with ALS [13–16] and was comparable to those in recent scRNA-seq studies in other diseases [18, 20]. Meanwhile, we could not provide the analysis comparing patients with and without cognitive impairment and with different onset sites due to the small sample size. Second, the difference in the numbers of patients between the non-rapid ALS and rapid ALS groups was relatively large. Third, longitudinal assessment was beyond the scope of this study. Additional evaluation in different stages would better clarify the temporal, progressive changes of immune profiles in ALS. Fourth, although not only the frequency but also the function of the immune cells such as Treg is important [37], we focused on their frequency in this study. Fifth, the evaluation of the CSF sample was beyond the scope of this study. Sixth, we did not measure neurofilament light chain with Simoa because of our limited budget.

Conclusions

In summary, this study revealed relationships between rapid progression and increase in Th17 against Treg, effector CD8 T cells against naïve CD8 T cells, and relevant proteins such as IL-17 A and KLRD1 (CD94) in the blood in ALS patients, suggesting these cell types together relate to disease progression in ALS.

Materials and methods

Experimental design

We aimed to identify immune cells and proteins that relate to ALS progression rate via scRNA-seq of PBMCs and high-throughput PEA-based immunoproteomic analysis of serum. Then, the clinical information was compared with scRNA-seq and proteomics data (Fig. 1A).

Participants

We conducted a screening involving 36 patients diagnosed with ALS and 10 healthy volunteers at Tokushima University Hospital in Tokushima, Japan, spanning from March 29, 2021, to October 30, 2022. To be eligible for inclusion in the study, patients had to meet the ALS diagnostic criteria established by the Gold Coast criteria [38] and have a disease duration of up to 2 years from the onset of symptoms. It is important to note that the patients' ages and sexes were carefully matched with those of the healthy participants. Table S8 lists the exclusion criteria for patients with ALS and healthy participants. We examined genetic background of the following genes: *ALS2*, *ANG*, *ANXA11*, *ATXN2*, *BNIP3L*, *C9orf72*,

CALCOCO2, *CBL*, *CCNF*, *CHCHD10*, *CHMP2B*, *CSF1R*, *CYLD*, *DAO*, *DCTN1*, *DYNLL1*, *ELP3*, *ERBB4*, *EWSR1*, *FIG4*, *FUS*, *GABARAP*, *GLE1*, *GRN*, *HDAC6*, *HNRNPA1*, *HNRNPA2B1*, *HNRPA2B1*, *KIF5A*, *LRP12*, *MAP1LC3A*, *MATR3*, *NBR1*, *NEFH*, *NEK1*, *OPTN*, *PFN1*, *PRPH*, *RNASE4*, *RNF19A*, *SETX*, *SIGMAR1*, *SKP1*, *SOD1*, *SPAST*, *SPG11*, *SPTLC1*, *SQSTM1*, *SS18L1*, *TAF15*, *TARDBP*, *TBK1*, *TFG*, *TIA1*, *TNFRSF11A*, *TNFSF11*, *TUBA4A*, *UBQLN2*, *VAPB*, *VAPBC*, and *VCP*. Patients with known pathogenic ALS variants were excluded beforehand from the analysis because the immunological profiles would be different from those of sporadic ALS. Rapid ALS was defined as a decrease in the ALSFRS-R score of ≥1.0 points per month (ΔALSFRS-R/month≥1), whereas non-rapid ALS was defined as a decrease in the ALSFRS-R score of <1.0 point per month (ΔALSFRS-R/month<1). As described below, we collected peripheral blood samples and conducted scRNA-seq and proteomic analyses. All study protocols were approved by the Ethics Committee of Tokushima University Hospital under protocol #3682. All clinical information was collected after patients provided written informed consent. The investigations were conducted following the principles of the Declaration of Helsinki.

Sample preparation

Peripheral blood samples were collected in Benoject II Vacuum Blood Collection Tube Sterilized Product VP-H100K (Terumo Corporation, Tokyo, Japan) from healthy volunteers and patients with ALS at Tokushima University Hospital. Ficoll-Hypaque (Lymphoprep™, Serumwerk Bernburg AG, Germany) density centrifugation prepared PBMCs, which were washed with phosphate-buffered saline (PBS) and resuspended in X-VIVO™ medium (LONZA, Basel, Switzerland) with 5% fetal bovine serum. PBMCs were resuspended in CELLBANKER 1 cryopreservation medium (Nippon Zenyaku Kogyo Ltd, Fukushima, Japan) and then stored at −80℃ until the library preparation. Serum samples were collected in 8.0 ml of Insepack tube (SEKISUI MEDICAL CO., LTD., Tokyo, Japan), centrifuged at 3,500 rpm for 10 min, aliquoted, and frozen at −80℃ within 20 min following collection.

Single-cell RNA-sequencing

PBMCs preparation, library preparation, and sequencing

Cryopreserved human PBMCs were rapidly thawed in a 37 °C water bath and washed with 1 × D-PBS (magnesium/calcium-free) containing 1% BSA. Cell collection was performed at 20 °C, with a centrifugation speed of 250 × g for 10 min using a swing-out rotor. After being washed three times, the cells were resuspended in an appropriate volume of D-PBS with 1% BSA. Subsequently, the cell suspension was passed through a Flowmi Cell Strainer with a pore size of 40 μm to eliminate any remaining larger particles. Cell count and viability were assessed using a hemacytometer with trypan blue staining.

We used scRNA-seq and the 10x Genomics (Pleasanton, CA) platform. The 10x Genomics Chromium controller was employed to load single-cell suspensions (10,000 cells) onto a chip to generate GEMs (Gel Bead-In-Emulsions). The Chromium Next GEM Single Cell 3' Reagent Kits v3.1 from 10x Genomics was used to prepare DNA libraries, following the manufacturer's instructions. Before sequencing, quality control of the prepared libraries was conducted using the 4200 TapeStation D1000 ScreenTape (Agilent, Santa Clara, CA) and the Qubit dsDNA Assay (Thermo Fisher Scientific, Waltham, MA). The gene expression libraries were sequenced on the DNBSEQ-G400 platform from MGI Tech (Shenzhen, China) at a depth of 50,000 reads per cell.

Data normalization

We employed the 10x Genomics Cell Ranger version 3 pipeline for primary analysis. The Cell Ranger "counts" software was utilized to convert Bcl files to FASTQ format. Subsequently, the FASTQ data underwent filtering and were mapped to the GRCh38 reference genome.

The secondary analysis used R version 4.0.2 with the Seurat version 3 package [39, 40]. To exclude data from low-quality cells and doublet cells, we utilized the Seurat and DoubletFinder packages [40]. The count data were subjected to normalization through a global-scaling normalization method, employing the Seurat function "LogNormalize," followed by log transformation using the Seurat function "NormalizeData." Variable features were selected by directly modeling the mean-variance relationship, utilizing the Seurat function "FindVariableFeatures." These selected variable features were then used to identify integration features through the Seurat function "SelectIntegrationFeatures." The integration features were applied for linear transformation and utilized in principal component analysis (PCA) by employing the Seurat functions "ScaleData" and "RunPCA," respectively.

Reciprocal PCA was performed using the top 50 principal components to identify anchors. The data were separated by anchor, and the batch features were extracted using the function 'SelectIntegrationFeatures' from the Seurat package and merged using the function 'IntegrateData' [41]. All scRNA-seq data generated in this study have been deposited in the Gene Expression Omnibus repository, accessible at http://www.ncbi.nlm.nih.gov/geo, under the accession number GSE244263.

Analysis

The integrated and normalized data underwent a linear transformation and PCA using Seurat functions

"ScaleData" and "RunPCA." To identify important principal components, an elbow plot was generated by plotting standard deviations of the principal components. These significant principal components were then used to perform uniform manifold approximation and projection (UMAP) visualization, achieved through the Seurat functions "ElbowPlot" and "RunUMAP."

The identification of cell types was carried out using these crucial principal components. First, cell similarities were calculated using a k-nearest neighbor graph based on the Euclidean distance in PCA space. The edge weights between any two cells were determined based on the shared overlap with their local neighborhoods using Jaccard's similarity, facilitated by the Seurat function "FindNeighbors." Subsequently, cell populations were divided through clustering, accomplished by assessing the similarities between cells using the Louvain algorithm and the Seurat function "FindClusters."

Furthermore, cell types within each cluster were identified by examining cell-type-specific marker expression profiles for each cluster (Table S9). Although NK cells are commonly classified into two functionally distinct subsets, i.e., $CD56^{bright}CD16^{-}$ and $CD56^{dim}CD16^{+}$, NK cells were clearly divided into three subsets based on the relative expression of CD16 and CD56 in our analysis ($CD16^{low}CD56^{high}$ for naïve NK cells, $CD16^{high}CD56^{low}$ for mature NK cells, and $CD16^{middle}CD56^{low}$ for activated NK cells) (Fig. S5). Activated NK cell subsets expressed CD247 (CD3zeta), suggesting enhanced activation and cytotoxic capacity through efficient signaling and interaction with other immune receptors. The resolution used was "Seurat's default value" and the cluster numbers before and after annotation were 22 and 23 respectively. The reason why the number of clusters increased after the annotation was that only CD4 T cell was extracted, reclustered, and subdivided (e.g., Th1, Th17) within it. The filter thresholds were "mitochondria genes < 15% and gene feature counts 500 ~ 4000" and the cell number "422,135 cells" used in the downstream analysis. Normalized gene expression levels of cell-type marker genes for each cell type are shown in UMAPs (Fig. S5) and a heatmap (Fig. S6). To identify DEGs between groups within each cell type, the nonparametric Wilcoxon rank sum test was employed, with the Seurat function "FindMarkers."

Gene expression levels were visualized within each cluster using violin plots via the Seurat function "VlnPlot." Differences in the frequencies of each cell type between groups were assessed using Tukey's HSD test with the "TukeyHSD" function in the stats (R default) package.

Correlation tests used the "cor.test" function from the stats (R default) package. Finally, scatter plots, boxplots, and bar plots were created in R using the ggplot2 package [36] for visualization.

Protein measurement

We employed the Olink Target 96 Inflammation and Olink Explore 384 Inflammation panels from Olink Proteomics (Uppsala, Sweden) to simultaneously quantify multiple human proteins associated with inflammation (Table S10) [21, 22]. This quantification was achieved using PEA technology (for more information, visit https://www.olink.com). PEA technology involves a pair of antibodies, each linked to unique oligonucleotides (proximity probes) and bound to their respective protein targets. These probes only hybridize with each other when they are near forming double-stranded DNA. The resulting complex is then detected and quantified using quantitative real-time PCR for the Olink Target 96 Inflammation panel or next-generation sequencing for the Olink Explore 384 Inflammation panel. The data were presented in normalized protein expression (NPX), which is an arbitrary unit on a $\log_2$-scale. NPX values represent relative expression rather than absolute protein levels. For proteins measured by next-generation sequencing, all items were selected for analysis. Regarding items measured solely by real-time PCR, we selected those with > 50% of the samples above the detection limit for analysis. A scatter plot of the first and second principal components in the PCA of serum proteome samples is shown in Fig. S7.

To identify DEPs between groups, we used Tukey's HSD test with the "TukeyHSD" function in the stats (R default) package. We visualized the results through volcano plots created in R using the ggplot2 and ggrepel packages [42, 43] for visualization. Correlation tests used the "cor.test" function from the stats (R default) package. Furthermore, serum pNfH levels were measured using an ELISA kit from EUROIMMUN (Lübeck, Germany) [44, 45].

To test the reproducibility of the measurement, the concentrations of IL-17 A, which was identified as one of the DEPs, were additionally assessed using the Simoa® IL-17 A Advantage PLUS kit (Catalog #104428; Quanterix, Billerica, MA) run on the Simoa® HD-X Analyzer (Quanterix), in the participants whose residual re-frozen samples were available (healthy controls, 9 of 10; non-rapid ALS patients, 20 of 23, rapid ALS patients, 7 of 7). The functional lower limit of quantification was 0.012 pg/ml. The samples except for one of the healthy controls were analyzed in duplicate. Samples were diluted 1:2 and distributed on 96-well plates. These measurements were performed according to the manufacturer's instructions at SEKISUI MEDICAL CO., LTD. The data were presented in the $\log_2$-transformed scale.

Statistical analysis

Microsoft R open software (version 4.0.2) or GraphPad Prism version 10 (GraphPad Software, Boston, MA)

were used for statistical analyses. The nonparametric Wilcoxon rank sum test identified DEGs in scRNA-seq, which was corrected for multiple tests using Bonferroni's test. Tukey's HSD for multiple testing was used to identify DEPs in serum proteome and the differences in the frequencies of each cell type between the groups. Pearson's correlation coefficient was used for correlation tests. A 2-sided $p<0.05$ was considered significant.

Abbreviations

ALS	Amyotrophic lateral sclerosis
ALSFRS-R	Revised Amyotrophic Lateral Sclerosis Functional Scale
CNS	Central nervous system
DEG	Differentially expressed gene
DEP	Differentially expressed protein
FC	Fold change
HSD	Honestly significant difference
IL-17A	Interleukin-17 A
KLRD1	Killer cell lectin-like receptor D1
KRT19	Keratin, type I cytoskeletal 19
NCF2	Neutrophil cytosol factor 2
NK	Natural killer
NPX	Normalized protein expression
PBMCs	Peripheral blood mononuclear cells
PBS	Phosphate-buffered saline
PCA	Principal component analysis
PEA	Proximity extension assay
scRNA-seq	Single-cell RNA-sequencing
Simoa	Single molecule array
TCR	T cell receptor
TFF2	Trefoil factor 2
Th17	T helper 17 cells
Treg	Regulatory T cells
UMAP	Uniform manifold approximation and projection
YTHDF3	YTH domain-containing family protein 3

Supplementary Information

The online version contains supplementary material available at https://doi.org/10.1186/s12974-024-03327-w.

Supplementary Material 1

Acknowledgements
Not applicable.

Author contributions
Conceptualization: T.I., K.F., Y.I. Methodology: T.I., K.F., Y.O., Y.I. Investigation: T.I., Y.O., Y.M., Y.I. Visualization: T.I., K.F., Y.O. Supervision: Y.I. Writing—original draft: T.I., K.F. Writing—review & editing: T.I., K.F., Y.O., D.W., S.M., Y.M., N.M., H.M., Y.K., Y.I.

Funding
Takeda Pharmaceutical Company Limited (YI). MHLW Research on rare and intractable diseases Program Grant Number JPMH23FC1008 (YI).

Data availability
All scRNA-seq data generated in this study have been deposited in the Gene Expression Omnibus repository, accessible at http://www.ncbi.nlm.nih.gov/geo, under the accession number GSE244263. All other data needed to evaluate the conclusions in the paper are present in the paper and/or the Supplementary Materials.

Declarations

Ethics approval and consent to participate
All study protocols were approved by the Ethics Committee of Tokushima University Hospital under protocol #3682. All clinical information was collected after patients provided written informed consent. The investigations were conducted following the principles of the Declaration of Helsinki.

Consent for publication
Not applicable.

Competing interests
TI, YO, DW, SM, and YK are employees of Takeda Pharmaceutical Company Limited.

Received: 1 October 2024 / Accepted: 18 December 2024
Published online: 27 December 2024

References

1. Feldman EL, Goutman SA, Petri S, Mazzini L, Savelieff MG, Shaw PJ, Sobue G. Amyotrophic lateral sclerosis. Lancet. 2020;400:1363–80.
2. Goyal NA, Berry JD, Windebank A, Staff NP, Maragakis NJ, van den Berg LH, Genge A, Miller R, Baloh RH, Kern R, Gothelf Y, Lebovits C, Cudkowicz M. Addressing heterogeneity in amyotrophic lateral sclerosis CLINICAL TRIALS. Muscle Nerve. 2020;62:156–66.
3. Thonhoff JR, Simpson EP, Appel SH. Neuroinflammatory mechanisms in amyotrophic lateral sclerosis pathogenesis. Curr Opin Neurol. 2018;31:635–9.
4. Lyon MS, Wosiski-Kuhn M, Gillespie R, Caress J, Milligan C. Inflammation, Immunity, and amyotrophic lateral sclerosis: I. Etiology and pathology. Muscle Nerve. 2019;59:10–22.
5. Henkel JS, Beers DR, Wen S, Rivera AL, Toennis KM, Appel JE, Zhao W, Moore DH, Powell SZ, Appel SH. Regulatory T-lymphocytes mediate amyotrophic lateral sclerosis progression and survival. EMBO Mol Med. 2013;5:64–79.
6. Beers DR, Zhao W, Wang J, Zhang X, Wen S, Neal D, Thonhoff JR, Alsuliman AS, Shpall EJ, Rezvani K, Appel SH. ALS patients' regulatory T lymphocytes are dysfunctional, and correlate with disease progression rate and severity. JCI Insight. 2017;2:1–14.
7. Sheean RK, McKay FC, Cretney E, Bye CR, Perera ND, Tomas D, Weston RA, Scheller KJ, Djouma E, Menon P, Schibeci SD, Marmash N, Yerbury JJ, Nutt SL, Booth DR, Stewart GJ, Kiernan MC, Vucic S, Turner BJ. Association of regulatory T-cell expansion with progression of amyotrophic lateral sclerosis: a study of humans and a transgenic mouse model. JAMA Neurol. 2018;75:681–9.
8. Murdock BJ, Zhou T, Kashlan SR, Little RJ, Goutman SA, Feldman EL. Correlation of peripheral immunity with rapid amyotrophic lateral sclerosis progression. JAMA Neurol. 2017;74:1446–54.
9. Yazdani S, Seitz C, Cui C, Lovik A, Pan L, Piehl F, Pawitan Y, Kläppe U, Press R, Samuelsson K, Yin L, Vu TN, Joly AL, Westerberg LS, Evertsson B, Ingre C, Andersson J, Fang F. T cell responses at diagnosis of amyotrophic lateral sclerosis predict disease progression. Nat Commun. 2022;13:1–13.
10. Rentzos M, Evangelopoulos E, Sereti E, Zouvelou V, Marmara S, Alexakis T, Evdokimidis I. Alterations of T cell subsets in ALS: a systemic immune activation? Acta Neurol Scand. 2012;125:260–4.
11. Rolfes L, Schulte-Mecklenbeck A, Schreiber S, Vielhaber S, Herty M, Marten A, Pfeuffer S, Ruck T, Wiendl H, Gross CC, Meuth SG, Boentert M, Pawlitzki M. Amyotrophic lateral sclerosis patients show increased peripheral and intrathecal T-cell activation. Brain Commun. 2021;3:fcab157.
12. Staats KA, Borchelt DR, Tansey MG, Wymer J. Blood-based biomarkers of inflammation in amyotrophic lateral sclerosis. Mol Neurodegener. 2022;17:11.
13. Jin M, Günther R, Akgün K, Hermann A, Ziemssen T. Peripheral proinflammatory Th1/Th17 immune cell shift is linked to disease severity in amyotrophic lateral sclerosis. Sci Rep. 2020;10:5941.
14. Saresella M, Piancone F, Tortorella P, Marventano I, Gatti A, Caputo D, Lunetta C, Corbo M, Rovaris M, Clerici M. T helper-17 activation dominates the immunologic milieu of both amyotrophic lateral sclerosis and progressive multiple sclerosis. Clin Immunol. 2013;148:79–88.
15. Fiala M, Chattopadhay M, La Cava A, Tse E, Liu G, Lourenco E, Eskin A, Liu PT, Magpantay L, Tse S, Mahanian M, Weitzman R, Tong J, Nguyen C, Cho T, Koo P, Sayre J, Martinez-Maza O, Rosenthal MJ, Wiedau-Pazos M. IL-17A is increased

in the serum and in spinal cord CD8 and mast cells of ALS patients. J Neuroinflammation. 2010;7:76.
16. Rentzos M, Rombos A, Nikolaou C, Zoga M, Zouvelou V, Dimitrakopoulos A, Alexakis T, Tsoutsou A, Samakovli A, Michalopoulou M, Evdokimidis J. Interleukin-17 and interleukin-23 are elevated in serum and cerebrospinal fluid of patients with ALS: a reflection of Th17 cells activation? Acta Neurol Scand. 2010;122:425–9.
17. Furukawa T, Matsui N, Fujita K, Nodera H, Shimizu F, Miyamoto K, Takahashi Y, Kanda T, Kusunoki S, Izumi Y, Kaji R. CSF cytokine profile distinguishes multifocal motor neuropathy from progressive muscular atrophy. Neurol Neuroimmunol NeuroInflammation. 2015;2:e138.
18. Nehar-Belaid D, Hong S, Marches R, Chen G, Bolisetty M, Baisch J, Walters L, Punaro M, Rossi RJ, Chung CH, Huynh RP, Singh P, Flynn WF, Tabanor-Gayle JA, Kuchipudi N, Mejias A, Collet MA, Lucido AL, Palucka K, Robson P, Lakshminarayanan S, Ramilo O, Wright T, Pascual V, Banchereau JF. Mapping systemic lupus erythematosus heterogeneity at the single-cell level. Nat Immunol. 2020;21:1094–106.
19. Perez RK, Gordon MG, Subramaniam M, Kim MC, Hartoularos GC, Targ S, et al. Single-cell RNA-seq reveals cell type-specific molecular and genetic associations to lupus. Science. 2022;376:eabf1970.
20. Wu X, Liu Y, Jin S, Wang M, Jiao Y, Yang B, Lu X, Ji X, Fei Y, Yang H, Zhao L, Chen H, Zhang Y, Li H, Lipsky PE, Tsokos GC, Bai F, Zhang X. Single-cell sequencing of immune cells from anticitrullinated peptide antibody positive and negative rheumatoid arthritis. Nat Commun. 2021;12:4977.
21. Wik L, Nordberg N, Broberg J, Björkesten J, Assarsson E, Henriksson S, Grundberg I, Pettersson E, Westerberg C, Liljeroth E, Falck A, Lundberg M. Proximity extension assay in combination with next-generation sequencing for high-throughput proteome-wide analysis. Mol Cell Proteom. 2021;20:100168.
22. Sun BB, Chiou J, Traylor M, Benner C, Hsu YH, Richardson TG, Surendran P, Mahajan A, Robins C, Vasquez-Grinnell SG, Hou L, Kvikstad EM, Burren OS, Davitte J, Ferber KL, Gillies CE, Hedman ÅK, Hu S, Lin T, Mikkilineni R, Pendergrass RK, Pickering C, Prins B, Baird D, Chen CY, Ward LD, Deaton AM, Welsh S, Willis CM, Lehner N, Arnold M, Wörheide MA, Suhre K, Kastenmüller G, Sethi A, Cule M, Raj A, Burkitt-Gray L, Melamud E, Black MH, Fauman EB, Howson JMM, Kang HM, McCarthy MI, Nioi P, Petrovski S, Scott RA, Smith EN, Szalma S, Waterworth DM, Mitnaul LJ, Szustakowski JD, Gibson BW, Miller MR, Whelan CD. Plasma proteomic associations with genetics and health in the UK Biobank. Nature. 2023;622:329–38.
23. Gunturi A, Berg RE, Forman J. The role of CD94/NKG2 in innate and adaptive immunity. Immunol Res. 2004;30:29–34.
24. Gunturi A, Berg RE, Forman J. Preferential survival of CD8 T and NK cells expressing high levels of CD94. J Immunol. 2003;170:1737–45.
25. Borrego F, Masilamani M, Marusina AI, Tang X, Coligan JE. The CD94/NKG2 family of receptors: from molecules and cells to clinical relevance. Immunol Res. 2006;35:263–78.
26. Martinelli I, Zucchi E, Simonini C, Gianferrari G, Bedin R, Biral C, Ghezzi A, Fini N, Carra S, Mandrioli J. SerpinA1 levels in amyotrophic lateral sclerosis patients: an exploratory study. Eur J Neurol. 2024;31:e16054.
27. DICE (database of immune cell expression, expression quantitative trait loci [eQTLs], and epigenomics). https://dice-database.org/genes/RP11-386I14.4. Accessed 16 December 2024.
28. Mills KHG. IL-17 and IL-17-producing cells in protection versus pathology. Nat Rev Immunol. 2023;23:38–54.
29. Nardo G, Trolese MC, Verderio M, Mariani A, de Paola M, Riva N, Dina G, Panini N, Erba E, Quattrini A, Bendotti C. Counteracting roles of MHCI and $CD8^+$ T cells in the peripheral and central nervous system of ALS $SOD1^{G93A}$ mice. Mol Neurodegener. 2018;13:42.
30. Coque E, Salsac C, Espinosa-Carrasco G, Varga B, Degauque N, Cadoux M, Crabé R, Virenque A, Soulard C, Fierle JK, Brodovitch A, Libralato M, Végh AG, Venteo S, Scamps F, Boucraut J, Laplaud D, Hernandez J, Gergely C, Vincent T, Raoul C. Cytotoxic $CD8^+$ T lymphocytes expressing ALS-causing SOD1 mutant selectively trigger death of spinal motoneurons. Proc Natl Acad Sci U S A. 2019;116:2312–7.
31. Campisi L, Chizari S, Ho JSY, Gromova A, Arnold FJ, Mosca L, Mei X, Fstkchyan Y, Torre D, Beharry C, Garcia-Forn M, Jiménez-Alcázar M, Korobeynikov VA, Prazich J, Fayad ZA, Seldin MM, De Rubeis S, Bennett CL, Ostrow LW, Lunetta C, Squatrito M, Byun M, Shneider NA, Jiang N, La Spada AR, Marazzi I. Clonally expanded CD8 T cells characterize amyotrophic lateral sclerosis-4. Nature. 2022;606:945–52.
32. Jabri B, Selby JM, Negulescu H, Lee L, Roberts AI, Beavis A, Lopez-Botet M, Ebert EC, Winchester RJ. TCR specificity dictates CD94/NKG2A expression by human CTL. Immunity. 2002;17:487–99.
33. Gumá M, Busch LK, Salazar-Fontana LI, Bellosillo B, Morte C, García P, López-Botet M. The CD94/NKG2C killer lectin-like receptor constitutes an alternative activation pathway for a subset of $CD8^+$ T cells. Eur J Immunol. 2005;35:2071–80.
34. Bielekova B, Catalfamo M, Reichert-Scrivner S, Packer A, Cerna M, Waldmann TA, McFarland H, Henkart PA, Martin R. Regulatory $CD56^{bright}$ natural killer cells mediate immunomodulatory effects of IL-2Rα-targeted therapy (daclizumab) in multiple sclerosis. Proc Natl Acad Sci U S A. 2006;103:5941–6.
35. McGill RB, Steyn FJ, Ngo ST, Thorpe KA, Heggie S, Ruitenberg MJ, Henderson RD, McCombe PA, Woodruff TM. Monocytes and neutrophils are associated with clinical features in amyotrophic lateral sclerosis. Brain Commun. 2020;2:fcaa013.
36. Fu X, He Y, Xie Y, Lu Z. A conjoint analysis of bulk RNA-seq and single-nucleus RNA-seq for revealing the role of ferroptosis and iron metabolism in ALS. Front Neurosci. 2023;17:1113216.
37. Olson KE, Mosley RL, Gendelman HE. The potential for treg-enhancing therapies in nervous system pathologies. Clin Exp Immunol. 2023;211:108–21.
38. Shefner JM, Al-Chalabi A, Baker MR, Cui LY, de Carvalho M, Eisen A, Grosskreutz J, Hardiman O, Henderson R, Matamala JM, Mitsumoto H, Paulus W, Simon N, Swash M, Talbot K, Turner MR, Ugawa Y, van den Berg LH, Verdugo R, Vucic S, Kaji R, Burke D, Kiernan MC. A proposal for new diagnostic criteria for ALS. Clin Neurophysiol. 2020;131:1975–8.
39. Butler A, Hoffman P, Smibert P, Papalexi E, Satija R. Integrating single-cell transcriptomic data across different conditions, technologies, and species. Nat Biotechnol. 2018;36:411–20.
40. McGinnis CS, Murrow LM, Gartner ZJ. DoubletFinder: Doublet detection in single-cell RNA sequencing data using artificial nearest neighbors. Cell Syst. 2019;8:329–e3374.
41. Stuart T, Butler A, Hoffman P, Hafemeister C, Papalexi E, Mauck WM 3rd, Hao Y, Stoeckius M, Smibert P, Satija R. Comprehensive integration of single-cell data. Cell. 2019;177:1888–902.e21.
42. Wickham H. ggplot2: Elegant graphics for data analysis. New York: Springer; 2016.
43. Slowikowski K. ggrepel: Automatically Position Non-Overlapping Text Labels with 'ggplot2'. 2020. https://cran.r-project.org/package=ggrepel. Accessed 16 December 2024.
44. De Schaepdryver M, Jeromin A, Gille B, Claeys KG, Herbst V, Brix B, Van Damme P, Poesen K. Comparison of elevated phosphorylated neurofilament heavy chains in serum and cerebrospinal fluid of patients with amyotrophic lateral sclerosis. J Neurol Neurosurg Psychiatry. 2018;89:367–73.
45. Heckler I, Venkataraman I. Phosphorylated neurofilament heavy chain: a potential diagnostic biomarker in amyotrophic lateral sclerosis. J Neurophysiol. 2022;127:737–45.

Publisher's note